



A new method based on low background instrumental neutron activation analysis for major, trace and ultra-trace element determination in atmospheric mineral dust from polar ice cores



Giovanni Baccolo ^{a, b, c, *}, Massimiliano Clemenza ^{c, d}, Barbara Delmonte ^b, Niccolò Maffezzoli ^e, Massimiliano Nastasi ^{c, d}, Ezio Previtali ^{c, d}, Michele Prata ^f, Andrea Salvini ^f, Valter Maggi ^{b, c}

^a Graduate School in Polar Sciences, University of Siena, Via Laterina 8, 53100, Siena, Italy

^b Department of Environmental Sciences, University of Milano-Bicocca, P.zza della Scienza 1, 20126, Milano, Italy

^c INFN, Section of Milano-Bicocca, P.zza della Scienza 3, 20126, Milano, Italy

^d Department of Physics, University of Milano-Bicocca, P.zza della Scienza 3, 20126, Milano, Italy

^e Centre for Ice and Climate, Niels Bohr Institute, Juliane Maries Vej, 30, 2100, Copenhagen, Denmark

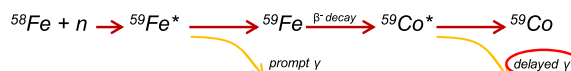
^f LENA, University of Pavia, Pavia, Italy

HIGHLIGHTS

- A new method based on neutron activation for the multi-elemental characterization of atmospheric dust entrapped in polar ice cores is proposed.
- 37 elements were quantified in µg size dust samples with detection limits ranging from 10⁻¹³ to 10⁻⁶ g.
- A low background approach and a clean analytical protocol improved INAA performances to unprecedented levels for multi-elemental analyses.

GRAPHICAL ABSTRACT

Low Background INAA applied on dust from polar ice cores



Limits of Detection (ng)

Na 0.7	Mg 30	Al 4	Si 3,000	K 25	Ca 200	Sc 6·10 ⁻⁴	Ti 30	V 0.1	Cr 0.3
Mn 0.8	Fe 8	Ni 0.6	Co 0.006	Zn 0.1	As 0.03	Se 0.01	Rb 0.8	Sr 2	
Sb 0.01	Cs 0.005	Ba 10	La 0.08	Ce 0.09	Nd 0.2	Sm 0.005	Eu 0.005	Tb 0.003	
Ho 0.004	Tm 0.001	Yb 0.02	Lu 0.001	Hf 0.06	Ta 0.03	Hg 0.009	Th 0.04	U 0.09	

ARTICLE INFO

Article history:

Received 27 January 2016

Received in revised form

31 March 2016

Accepted 5 April 2016

Available online 9 April 2016

Keywords:

Low background neutron activation analysis

Ultra-trace analysis

Ice core

Atmospheric mineral dust

ABSTRACT

Dust found in polar ice core samples present extremely low concentrations, in addition the availability of such samples is usually strictly limited. For these reasons the chemical and physical analysis of polar ice cores is an analytical challenge. In this work a new method based on low background instrumental neutron activation analysis (LB-INAA) for the multi-elemental characterization of the insoluble fraction of dust from polar ice cores is presented. Thanks to an accurate selection of the most proper materials and procedures it was possible to reach unprecedented analytical performances, suitable for ice core analyses. The method was applied to Antarctic ice core samples. Five samples of atmospheric dust (µg size) from ice sections of the Antarctic Talos Dome ice core were prepared and analyzed. A set of 37 elements was quantified, spanning from all the major elements (Na, Mg, Al, Si, K, Ca, Ti, Mn and Fe) to trace ones, including 10 (La, Ce, Nd, Sm, Eu, Tb, Ho, Tm, Yb and Lu) of the 14 natural occurring

* Corresponding author. Graduate School in Polar Sciences, University of Siena, Via Laterina 8, 53100, Siena, Italy.

E-mail address: giovanni.baccolo@mib.infn.it (G. Baccolo).

lanthanides. The detection limits are in the range of 10^{-13} – 10^{-6} g, improving previous results of 1–3 orders of magnitude depending on the element; uncertainties lies between 4% and 60%.

© 2016 Elsevier B.V. All rights reserved.

1. Introduction

Ice cores from polar ice caps represent a unique climatic archive for the past [1,2]. Through the analysis of the chemical and physical properties of ice and its content it is possible to reconstruct several climatic and environmental parameters. Among the climatic proxies retrievable from ice cores an important role is played by the atmospheric mineral dust (onward “dust”) entrapped in the ice and snow layers. The dust cycle is strictly connected to the climate: climate affects the production, transport and deposition of dust, but it is influenced by dust itself [3]. The determination of the chemical composition of dust retrieved from ice cores is a useful tool for paleoclimatic reconstructions. An immediate information linked to the composition of the dust deposited in remote areas as Antarctica is its provenance. The identification of geochemical correlations between dust samples extracted from ice cores and samples collected from potential source areas allows recognizing the main sources of dust in the different climatic periods. This is essential for the understanding of the past atmospheric circulation and for the validation of the atmospheric models [4,5]. Another important issue related to dust composition is its role within the biogeochemical cycles of some elements and the indirect influence on climate [6,7].

From the analytical point of view the physical and chemical analysis of polar ice core dust is a challenge. The two limiting factors are the extremely reduced concentration of dust within the ice [8] and the limited availability of ice core samples. Up to now several methods have been specifically developed for the characterization of ice core dust. Focusing the attention to compositional and provenance studies, isotopical analyses play a key role, with particular regard to Sr, Nd and Pb for which thermal ionization mass spectrometry is the reference technique [9–12], despite also inductively coupled plasma sector field MS (ICP-SFMS) and multi collector ICP-MS were successfully applied for the analysis of Sr, Nd, Pb and other radiogenic isotopes [13,14]. Other successful attempts to define a fingerprint or to recognize a temporal shift of the dust origin in polar ice core samples were made using selected elements like rare earth elements [15,16] (REE), platinum group elements [17] or other trace elements [18–22], mainly determined by ICP-SFMS. Major elements (Na, Mg, Al, Si, K, Ca, Ti, Mn and Fe) composition of dust entrapped in polar ice was investigated through different techniques: proton induced x-ray emission and proton induced γ -ray emission [23], synchrotron x-ray fluorescence and x-ray absorption near edge structure [24], total X-ray reflection fluorescence [25] and laser ablation ICP-MS [26–28].

We propose a new method based on low background instrumental neutron activation analysis (LB-INAA) for the elemental characterization of the insoluble fraction of atmospheric dust entrapped in polar ice cores. Instrumental neutron activation analysis (INAA) is a well established technique for elemental analysis, especially dealing with complex samples, as geological and environmental ones, since it is poorly affected by recovery and interference issues [29–31]. This is not the first attempt to apply INAA to bare snow and ice [32–34] and neither to ice cores [35–38]. But the detection limits reported in these works are not suitable for an accurate geochemical characterization of the atmospheric dust found in polar ice cores. Only few elements were

quantified (in most cases Na, Al and Cl) and high mass samples were requested. We tried to overcome these limitations applying a low background approach. When the radioactivity of the activated samples presents very low levels it is mandatory to apply passive and/or active methods to reduce the radioactive background. Some of the most common solutions are the selection of radio-pure shielding and detectors, the installation of the apparatus in an underground laboratory for a reduction of the cosmic radiation and the application of active shielding systems [39,40]. We developed a LB-INAA method specifically suited for the analysis of the atmospheric dust found in polar ice cores. For the first time appropriate levels of sensitivity, precision and accuracy were reached, leading to an accurate determination of 37 elements in μg -size dust samples.

2. Materials and methods

2.1. Apparatus

According to INAA samples are exposed to a neutron flux. The interaction between the atomic nuclei which constitute the samples and the neutrons induces nuclear reactions and the production of radioactive nuclei. When the latter decay it becomes possible to observe the emission of radiations and particles. INAA focuses the attention on the neutron capture reactions and on the emission of γ -rays, whose intensity and energy allow determining the elemental composition of the sample. The irradiation of the ice core dust samples was carried out at LENA (Applied Nuclear Energy Laboratory, Pavia, Italy), where a Triga Mark II nuclear reactor is installed. Within this facility we got access to 2 different lines, the “Rabbit” channel and the “Lazy Susan” one [41]. The “Rabbit” channel is designed for fast irradiations: it allows introducing the samples in the reactor for short times one by one; its application is the determination of short-lived radionuclides. The “Lazy Susan” channel was used for long irradiations and the observation of medium- and long-lived radionuclides, for further details see Table 2.

Two p-type high purity germanium detectors were used for the acquisition of the γ -spectra: a coaxial detector and a well-type one. Both are designed for low radioactive measurements, an essential requisite considering the reduced activity induced in the samples. To minimize the intrinsic radioactivity of the instruments only high radio-purity copper and aluminum and low cobalt content stainless steel were used for the internal parts of the detectors. In addition the preamplifier, the high-voltage filters, the cryogenic pump and the preamplifier were not placed near the detectors, where they could have been responsible of a radiation background increase. The detectors were also shielded from the environmental radiations using high purity lead (low ^{210}Pb content) and copper ingots. These solutions allowed to reach a radioactive background suitable for low-background measurements [42] and for the selection of materials used in rare event physics experiments [43,44]. The coaxial detector was used for the acquisition of the data concerning the short-lived radionuclides; it is installed at LENA, its relative efficiency is 30% and its energy resolution at the 1.332 MeV γ -line of ^{60}Co is 1.8 keV FWHM (full width half maximum). All the successive acquisitions concerning medium- and long-lived radionuclides,

were performed using the well-type detector, installed at the Radioactivity Laboratory of the University Milano-Bicocca. Its near 4π geometry allows an high efficiency (total active volume 350 cm^3), the energy resolution of this detector at the 1.332 MeV γ -line is 2.2 KeV FWHM.

2.2. Materials and reagents

Dealing with ice cores analyses particular care must be paid to avoid any contamination, which could potentially interferes with the considered analytes. Materials and cleaning procedures were selected after having carried out an accurate selection [45]. PTFE filter membranes ($0.45\ \mu\text{m}$ pore size, 11.3 mm diameter, Millipore[®]), rinsed for one month in double distilled ultrapure 1 M HNO_3 were used to extract the dust from the meltwater. Also the polyethylene vials (1 mL volume) used for the sample storing during irradiations and data acquisition were similarly treated. The filtration of meltwater samples from ice cores was carried out using a filtration system, specifically dedicated to the preparation of ice core samples, coupled with a vacuum pump. Plastic and glass parts of the system getting in touch with the filters were rinsed with nitric acid for 4–5 weeks. All acid rinsed materials were richly washed with MilliQ (Millipore[®]) water just before sample filtering. This precaution is of great importance: an acid environment could lead to a forced dissolution of mineral dust particles. Standard reference materials (RM) from NIST (1645, 2704, 2709a and 2710) and from USGS (AGV2 and BCR2) were used for calibration and neutron flux monitoring purposes.

2.3. Samples

Five samples from TALDICE were prepared and measured. TALDICE is a 1620 m long ice core drilled at Talos Dome (East Antarctica, Ross Sea sector, $159^\circ 11' \text{ E}$, $72^\circ 49' \text{ S}$) covering the last 150 kyr [46,47]. Samples, named TD1- TD2- TD3- TD4-TD5, were prepared using 69 sections of the core. The depth interval covered by the samples spans between 669 m and 1477 m, corresponding to a time interval from 11.600 years BP to >150.000 years BP. The dust content of each section was determined through Coulter counter technique (CC) measurement [48]. The estimated dust mass deposited on the filters ranges from 17 to $31\ \mu\text{g}$. For further details about the samples see Table 1 and the Supplementary material. The preparation of the samples was carried out at EUROCOLD laboratory (European Cold Laboratories Facilities, University of Milano-Bicocca) in a Class 1000 clean room. Ice samples were decontaminated removing the external ice according to Delmonte et al. [48]. The decontaminated ice was melted in clean containers under a Class 100 laminar flow bench and divided into two aliquots, one (7–8 g) for CC measurements and the remnant one for LB-INAA. LB-INAA was performed on the samples obtained merging and filtering several aliquots, in order to obtain an adequate amount of dust. 7 blank PTFE filters were prepared and analyzed following the same procedure adopted for SRMs and samples. For each blank filter 300 mL of MilliQ water were filtered to reproduce the filtration. It is

important to note that after the irradiation the contamination risk dramatically drops down, since the radionuclides used to determine the elemental masses are not naturally occurring. Previous analyses revealed a significant contamination of the vials used to store the samples [45], despite they were cleaned following the same procedure adopted for the membranes. For this reason irradiated filters were removed from irradiated vials just after the irradiation and placed in clean non-irradiated vials. In this way only the radioactive contribution associated to the filtered dust and to the membranes was considered (see Fig. 1).

2.4. Irradiations and γ -analysis

In order to maximize the activation of our samples long irradiation times were settled. Two irradiations were carried out: a short irradiation for the detection of short-lived radionuclides and a longer one for medium- and long-lived radionuclides. 5 acquisitions of the γ -spectra were performed for each sample, 2 after the short irradiation and 3 after the long one. More details about irradiations, γ -acquisitions and the observed nuclear reactions, are reported in Table 2 and in the Supplementary material. Some spectra are presented in Fig. 1.

2.5. Calculations

The determination of the elemental masses was carried out comparing the radioactive activities of RMs and samples. According to this relative method it is not necessary to consider neutron flux, neutron capture cross sections, isotopic abundances, detector efficiencies, acquisition geometry, branching ratios, neutron and γ -rays self-shielding effects. Also uncertainties associated to these parameters are neglected. Specific activities for each element (A_{spec} , $\text{counts s}^{-1} \mu\text{g}^{-1}$) are calculated using RMs, following Eq. (1), where A is the net count area of the considered photopeak, t_{acq} is the

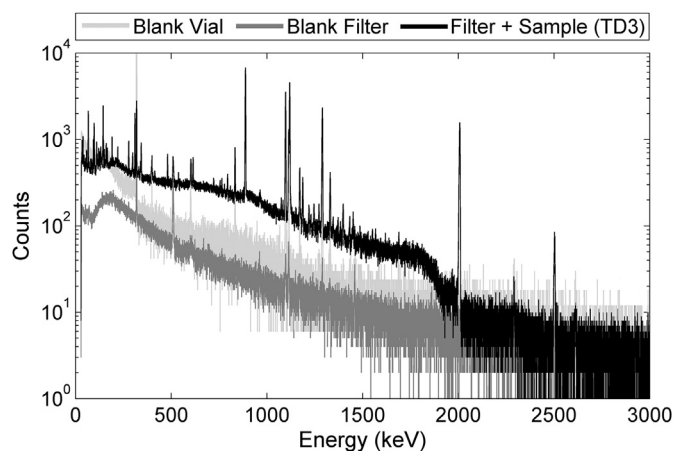


Fig. 1. γ -spectra relative to a blank filter, to a sample and to a polyethylene vial are compared. Data were corrected in order to make them fully comparable.

Table 1

Main information about the samples. The age of ice was taken from Veres et al. [47]. Filtered volume refers to total water volume filtered for each sample. Filtered dust mass (from CC measurements) refers to the dust fraction whose diameter lies between 1 and $10\ \mu\text{m}$. Dust mass errors depend on CC measurements.

Sample	Depth (m)	Age (Kyr B.P.)	Filtered vol. (mL)	Filtered dust mass (μg)
TD1	669–798	11.6–16.3	676	29 ± 2
TD2	1211–1256	52.9–59.4	198	17 ± 1
TD3	1260–1299	60.0–70.5	199	28 ± 3
TD4	1423–1441	136.5–150.0	204	30 ± 2
TD5	1445–1477	>150.0	280	31 ± 3

Table 2
Timings and details of the irradiations and acquisitions, neutron fluxes from Borio di Tigliole et al. [49].

Irradiation	Irradiation time	Neutron flux (n cm ² s ⁻¹)	Cooling time	Acquisition time	Obs. Elements	
Short irradiation	RMs: 300 s	(7.40 ± 0.95) · 10 ¹²	≈ 130 s	400 s	Mg, Al, Si, Ti, V	
	Samples: 900 s					
Long irradiation	60 h	(2.40 ± 0.24) · 10 ¹²	≈ 900 s	400 s	Mg, Ti, Mn	
				1–8 d	RMs: ≈ 1 h	Na, K, Ca, As, Sb, Ba, La, Nd, Sm, Lu, W, U
				10–20 d	Samples: ≈ 6 h	
					Blanks: ≈ 14 h	
				20–100 d	RMs: ≈ 1 h	Cr, Sb, Ce, Sm, Ho, Yb, Hf, Th
					Samples: ≈ 1 d	
	Blanks: ≈ 1.5 d					
	RMs: ≈ 1 d	Sc, Cr, Fe, Co, Ni, Zn, Se, Rb, Sr, In, Sb, Cs, Ce, Eu, Tb, Tm, Yb, Hf, Ta, Hg, Th				
	Samples: ≈ 5–9 d					
	Blanks: ≈ 5–9 d					

acquisition time, λ is the decay constant of the considered radionuclide, t_c is the cooling time, K is a corrective factor which accounts for the radioactive decay occurring during the acquisition (see the [Supplementary material](#)) and $(m_{el})_{RM}$ is the known amount of the considered element in the RM expressed in μg . Sample activities (A_{sample} , counts s⁻¹) are determined using Eq. (2).

$$A_{\text{spec}} = \frac{\frac{A}{t_{\text{acq}}} \cdot e^{\lambda \cdot t_c} \cdot K}{(m_{el})_{RM}} \quad (1)$$

$$A_{\text{sample}} = \frac{A}{t_{\text{acq}}} \cdot e^{\lambda \cdot t_c} \cdot K \quad (2)$$

The elemental mass within the sample is determined comparing A_{sample} and A_{spec} , in accordance to Eq. (3).

$$(m_{el})_{\text{sample}} = \frac{A_{\text{sample}}}{A_{\text{spec}}} \quad (3)$$

In the case of the short irradiation it was necessary to apply a further correction to consider the different irradiation times of samples and RMs (see the [Supplementary material](#)). A complete presentation of INAA calculation and metrology is given in Greenberg et al. [50].

Energy peaks were recognized and fitted using a Gaussian function, after the subtraction of the radioactive background. This latter was fitted using the most proper polynomial function. Net integral areas of interest (the term A comparing in Eqs. (1) and (2)) were determined and used for the successive calculation steps. Uncertainties were quantified considering the following sources: weighing operations, instrumental dead time, peak area fitting and calculation, blank subtraction, RMs element concentration uncertainties. In the case of the short irradiation timing uncertainties and temporal fluctuations of the neutron flux were also taken into account [51]. In the case of Mg and Al also a correction for epithermal neutron reactions was necessary, since the production of ²⁷Mg and ²⁸Al is interfered by the following reactions associated to non-thermal neutrons: ²⁷Al(n,p)²⁷Mg, ²⁸Si(n,p)²⁸Al. The contribution of the interferences were evaluated irradiating high purity Al and Si. The final uncertainty budget for these elements kept into account this point. Detection limits (DL) were determined in accordance to Eq. (4), as proposed in Currie [52]: A_{DL} is the detection limit expressed in instrumental counts and $(A_{In})_B$ is the gross integral area of the blank observed in correspondence of the selected γ -energy. To obtain the DL expressed as mass it is necessary to combine Eqs. (3) and (4). Final DLs, reported in the [Supplementary material](#), were calculated as the average value of the 7 blanks.

$$A_{DL} = 2.71 + 4.65 \sqrt{(A_{In})_B} \quad (4)$$

3. Results and discussion

3.1. Blanks and detection limits

Blank filters analysis revealed a low contamination; the only detectable elements in the blank filters are the following: Na (0.4%), Al (0.5%), Sc (0.5%), Cr (15%), Fe (1%), Co (2%), Zn (7%), Hg (20%). Values in brackets represent the relative contributions of the blanks with respect to the samples. DLs are strictly related to the activation rate associated to each element. This latter depends on several factors: the isotopic abundance of the selected nuclide, its neutron capture cross section, the branching ratio of the considered γ -emission and the detector efficiency at that given γ -energy. In [Fig. 2b](#) the activation rate for each element is plotted against the corresponding DL. As expected DLs are negatively correlated to the activation rate. The elements presenting high activation rates show low DLs, in the range of 10⁻¹³–10⁻¹¹ g. Mg, K, Ca, Ti and Ba, characterized by low cross sections, present higher DLs, in the range of 10⁻⁹–10⁻⁷ g. Si is the only element whose DL is in the range of 10⁻⁶ g; this is related to the nuclear reaction used for the detection of this element (see the [Supplementary material](#)). In [Fig. 3](#) the DLs obtained within this work using LB-INAA are compared to DLs obtained through traditional INAA. For most of the elements the improvement in terms of sensitivity is evident. For many elements (Ni, Se, Rb, Sr, Cs, Nd, Tb, Yb, Lu, Ta, Hg, U) the improvement is greater than a factor of 500, while for other 10 elements it lies in the 10–500 range. These results are indicative of the great potential of LB-INAA as an analytical tool for the multi-elemental determination of trace- and ultra-trace elements in micro-size samples. It is important to note that these improvements concern multi-elemental analyses. Focusing the attention on a single or on few elements it is possible to obtain even lower DLs, for example adopting a coincidence counting scheme or radiochemical methods [37,43], but these approaches don't allow the determination of many elements at the same time.

3.2. Accuracy, precision and repeatability

The estimation of accuracy dealing with unconventional samples is a difficult task, mainly because it is not possible to find a proper reference material. We tried to bypass this point by using one aliquot (≈ 5 mg) of NIST standard RM 2710a to evaluate the accuracy of the method. It was irradiated following the same

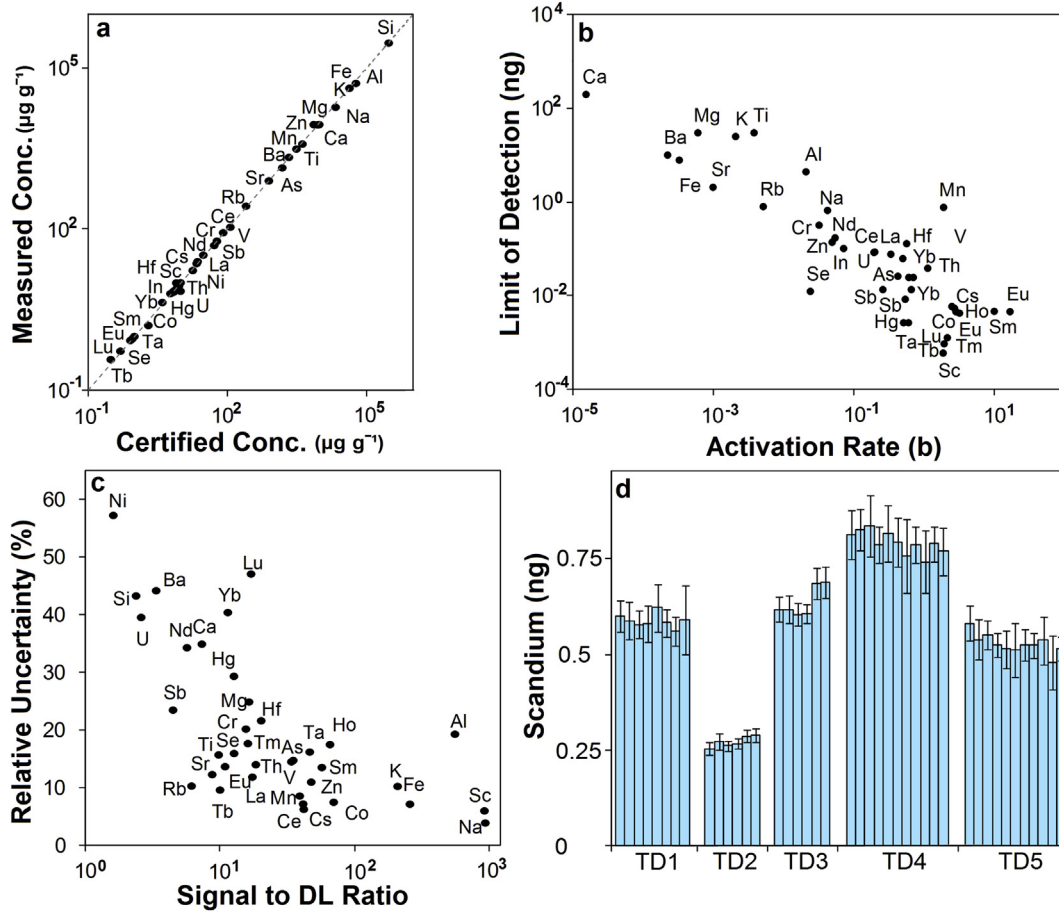


Fig. 2. Analytical results. Part a: certified vs. measured elemental concentrations of NIST standard RM 2710a. Part b: activation rate versus DLs; activation rates are expressed in barn (b), corresponding 10^{-26} m^2 and are normalized taking into account the isotopic abundance, the decay branching ratios and the detector efficiency at that energy. Si and Ni are not included because the nuclear reaction involved in their measurement is not a standard neutron capture. Part c: signal to DL ratio vs. average relative uncertainty. Part d: Sc elemental mass determined in the samples measured at different times.

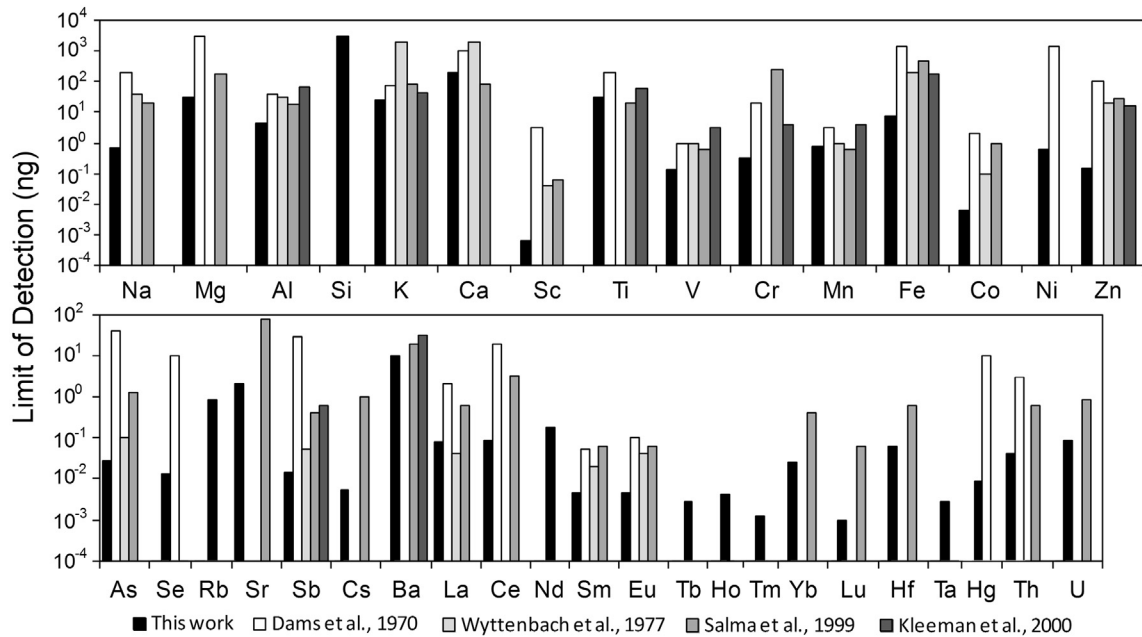


Fig. 3. The DLs obtained applying the method proposed in this work compared with traditional INAA applied to different sample typologies. Data were taken from Ref. [33] (Alpine ice) [53], (urban particulate matter) [54], (size-fractionated aerosols) and [55] (particulate matter emitted by motor vehicles).

procedure adopted for the other samples. Results are reported in Fig. 2a. Significant deviations, higher than 20%, are observed for Mg (+23%), Ni (+25%), Yb (−20%) and Hg (−30%).

Precision was evaluated through the uncertainties of sample measurements. Relative uncertainties range from less than 5% for Na to more than 50% for Ni as it is possible to see in Fig. 2c. This spread is due to the different signal to DL ratio, defined as the ratio between the average elemental amount within the samples and the respective DL. Fig. 4 refers to this point; 3 groups of elements whose signal to DL ratio respectively lie in the range 1–10, 10–100 and 100–1000 are presented. A significant decrease of precision occurs when the ratio approaches values near one. Elements with uncertainties higher than 20% are: Si (45%), Ca (35%), Cr (25%), Ni (60%), Sb (25%), Ba (45%), Nd (35%), Yb (40%), Lu (50%), Hg (30%), U (40%). To improve the precision for these elements it should be necessary to increase the signal to DL ratio by extending the irradiation time and/or the acquisition one or by retaining a higher amount of dust on the membranes.

The repeated determination of Sc at different times, using 2 γ -energies (889.3 and 1120.5 keV), was used to assess the repeatability of the method (see Fig. 2d). The time interval from the first to the last measurement span from 80 to 120 days depending on the sample; fluctuations are always smaller than 7%.

3.3. Sample composition

Elemental masses of the five samples are reported in the

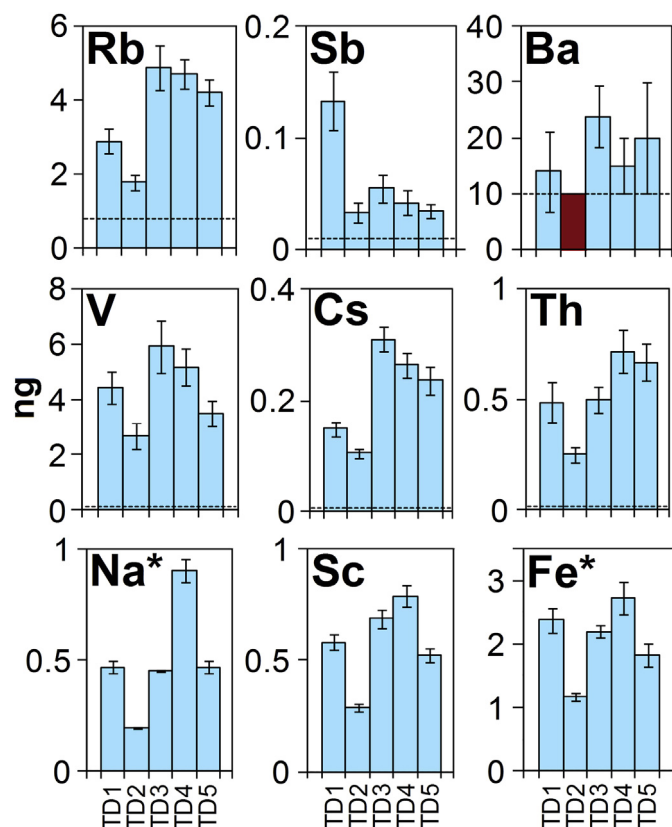


Fig. 4. Elemental masses determined in the samples. The dashed line refers to the DL; dark bars refers to samples presenting an elemental mass below the associated DL. 9 of the 37 observed elements are reported. In the first (second – third) row three elements whose signal to DL ratio lies between 1 and 10 (10 and 100–1000 and 1000) are reported. All values are expressed in ng, with the exception of Na and Fe, in this case values are expressed in μg .

Supplementary material. LB-INAA allowed measuring the mass of 37 elements within the dust deposited on the filters. Masses range from 10^{-11} g for many trace elements to 10^{-7} – 10^{-6} g for major elements. To the best of our knowledge this is the first measurement of Ni, Se, Hf, Ta and Th content in ice core samples.

In Fig. 5 the characterization of the samples is presented; major (Fig. 5a), rare earth (Fig. 5b), incompatible (as defined in Sun et al. [56], Fig. 5c) and volatile elements (Fig. 5d) are reported. Data are expressed using enrichment factors (EF) with respect to the average composition of the Upper Continental Crust [57], considering scandium as crustal reference (Sc-UCC). The crustal origin of the material deposited on the filters is confirmed by the EFs. For most of the elements the EFs present values near 1, revealing a composition similar to the UCC one, despite some elements (Ti, Ta and Hf) present an enrichment in most of the samples ($EF \approx 3$ –4). Ti, Ta and Hf all belong to the high field strength elements (HFSE), an elemental group characterized by very low aqueous solubility and high mechanical and chemical resistance. It has already been observed that HFSE can be enriched in atmospheric mineral dust as a consequence of weathering processes occurring during the atmospheric transport [58].

In the case of volatile elements (Fig. 5d), in particular Se and Hg, a merely crustal origin seems unlikely, since very high EFs are observed (in some cases higher than 100). Important natural sources for these volatile elements are volcanic activity, sea salt spray and marine biosphere [59,60]. All of these sources could be involved for explaining the enrichment observed in the TALDICE samples, since Talos Dome is not far from important active volcanoes (Mt Melbourne, Mt Erebus) and the Victoria Land coastal areas, where the biogenic emission of Se and Hg could be significant in relation to marine biochemistry and sea salt aerosol formation.

3.4. Comparison with ICP-SFMS

The analytical procedure proposed in this work finds as natural competitor ICP-SFMS, the most used technique for the multi-elemental characterization of ice cores [15–22]. LB-INAA is focused on the insoluble content of ice cores; classical ICP-SFMS, directly applied to melted ice, is more focused on the soluble elemental fraction. The investigation of the insoluble fraction through ICP-SFMS requires a complete mineralization of the samples. These differences are critical from a geochemical point of view, since the behavior of the elements is different when considering soluble or insoluble species. But the importance of this point is not only related to a geochemical perspective, also to a merely analytical one. Recent observations suggest that the traditional mineralization method, i.e. the addition of pure acid to melted ice, is not sufficient to obtain a complete recovery of the analytes, in particular of the fraction retained in the insoluble particles [61–66]. Several weeks or months could be necessary for a total dissolution of dust particles after the addition of acid to melted ice [66]. In this context our method could be useful to determine the total insoluble elemental budget of ice cores, since INAA is not affected by recovery problems and matrix effects, in particular dealing with small samples [50]. The only dust fraction which could be not retained by the filters is the one whose size is minor than membrane pores ($0.45 \mu\text{m}$), but this fraction in Antarctic dust is negligible [48]. LB-INAA could be used to define a reference for ICP-SFMS measurements on ice cores, allowing to quantify the recovery factors relative to the insoluble fraction. Despite these arguments ICP-SFMS present the undeniable advantage to make possible the analysis of hundreds of samples. The two techniques should be considered as complementary to each other. ICP-SFMS can lead to the construction of highly detailed time series focused on selected elements and

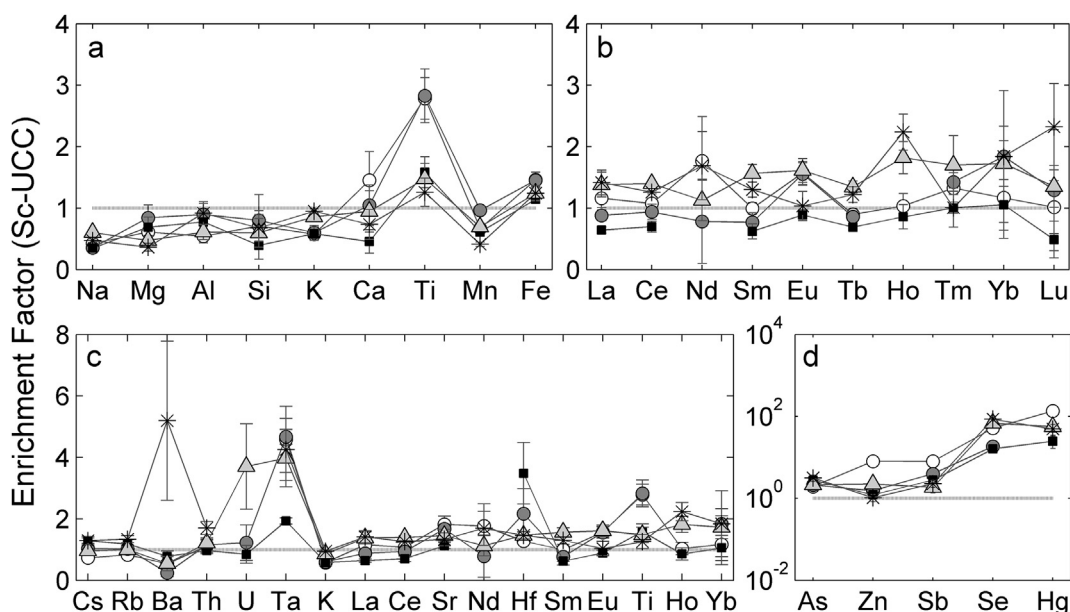


Fig. 5. The geochemical composition of the dust extracted from TALDICE. Part a: major elements. Part b: rare earth elements. Part c: incompatible elements. Part d: volatile elements. All values are expressed as enrichment factor with respect to the Sc-UCC. The samples are associated to the following series: TD1 (white circles), TD2 (grey circles), TD3 (black squares), TD4 (light grey triangles), TD5 (black stars).

in particular on their soluble and easy-solubilizable fractions. LB-INAA could be used for an accurate multi-elemental and geochemical analysis of selected insoluble atmospheric dust samples in specific climatic periods, determining more than 30 elements at the same time. A comparison of the different results could give important achievements in the understanding of the biogeochemical cycle of many elements, in particular in relation to their behavior as soluble or insoluble species.

4. Conclusions

A new method based on LB-INAA technique for the multi-elemental analysis of atmospheric mineral dust retrieved from polar ice cores was developed. Given the extremely low concentration of dust in polar ice the definition of the entire protocol focused the attention on the reduction of the contamination and on the improvement of the analytical performances, in particular the detection limits. These latter were improved of up to 3 orders of magnitude if compared to traditional methods based on INAA. This is an important achievement since neutron activation analysis, in the form of LB-INAA, could now be considered as a powerful tool, suitable for the multi-elemental analysis of trace and ultra-trace elements in μg -size samples. A first attempt to apply the technique was successfully carried out on five dust samples extracted from the Antarctic TALDICE ice core. The method proved to be able to determine 37 elements with different degrees of precision in samples consisting in 15–40 μg of atmospheric mineral dust extracted from a polar ice core. For Ni, Se, Hf, Ta and Th these are the first measurements carried out on ice core samples. Considering such a great number of elements it was possible to define an accurate and coherent geochemical fingerprint of the filtered material, inferring some preliminary but important features of the dust deposited at Talos Dome (East Antarctica). LB-INAA is a promising method; in the future it will be possible to apply it not only in the field of ice core science, but in the generic field of micro-chemistry.

Acknowledgements

The Talos Dome Ice core Project (TALDICE), a joint European programme, is funded by national contributions from Italy, France, Germany, Switzerland and the United Kingdom. Primary logistical support was provided by PNRA at Talos Dome. This is TALDICE publication no 44.

Appendix A. Supplementary data

Supplementary data related to this article can be found at <http://dx.doi.org/10.1016/j.aca.2016.04.008>.

References

- [1] Epica Community Members, *Nature* 429 (2004) 623–628.
- [2] North Greenland Ice Core Project Members, *Nature* 431 (2004) 147–151.
- [3] B.A. Maher, J.M. Prospero, D. Mackie, D. Gaiero, P.P. Hesse, Y. Balkanski, *Earth Sci. Rev.* 99 (2010) 61–97.
- [4] F. Li, P. Ginoux, V. Ramaswamy, *J. Geophys. Res. Atmos.* 113 (2008), <http://dx.doi.org/10.1029/2007JD009190>.
- [5] S. Albani, N. Mahowald, B. Delmonte, V. Maggi, G. Winckler, *Clim. Dynam.* 38 (2012) 1731–1755.
- [6] E.W. Wolff, H. Fischer, F. Fundel, U. Ruth, B. Twarloh, G.C. Littot, R. Mulvaney, R. Rothlisberger, M. de Angelis, C.F. Boutron, M. Hansson, U. Jonsell, M.A. Hutterli, F. Lambert, P. Kaufmann, B. Stauffer, T.F. Stocker, J.P. Steffensen, M. Bigler, M.L. Siggaard-Andersen, R. Udisti, S. Becagli, E. Castellano, M. Severi, D. Wagenbach, C. Barbante, P. Gabrielli, V. Gaspari, *Nature* 440 (2006) 491–496.
- [7] A. Martina-Garcia, D.M. Sigman, H. Ren, R.F. Anderson, M. Straub, D.A. Hodell, S.L. Jaccard, T.I. Eglinton, G.H. Haug, *Science* 343 (2014) 1347–1350.
- [8] F. Lambert, B. Delmonte, J.R. Petit, M. Bigler, P.R. Kaufmann, M.A. Hutterli, T.F. Stocker, U. Ruth, J.P. Steffensen, V. Maggi, *Nature* 452 (2008) 616–619.
- [9] I. Basile, F.E. Grousset, M. Revel, J.R. Petit, P.E. Biscaye, N.I. Barkov, *Earth Planet. Sc. Lett.* 146 (1997) 573–589.
- [10] P. Vallelonga, K. Van de Velde, J.P. Candelone, C. Ly, K.J.R. Rosman, C.F. Boutron, V.I. Morgan, D.J. Mackey, *Anal. Chim. Acta* 453 (2002) 1–12.
- [11] B. Delmonte, P.S. Andersson, M. Hansson, H. Shoberg, J.R. Petit, I. Basile-Doelsch, V. Maggi, *Geophys. Res. Lett.* 35 (2008), <http://dx.doi.org/10.1029/2008GL033382>.
- [12] C. Han, L.J. Burn-Nunes, K. Lee, C. Chang, J. Kang, Y. Han, S. Do Hur, S. Hong, *Talanta* 140 (2015) 20–28.
- [13] M. Krachler, J. Zheng, D. Fischer, W. Shotyk, *Anal. Chem.* 76 (2004) 5510–5517.
- [14] S.M. Aciego, B. Bourdon, M. Lupker, J. Rickli, *Chem. Geol.* 266 (2009) 194–204.

- [15] P. Gabrielli, C. Barbante, C. Turetta, A. Marteel, C. Boutron, G. Cozzi, W. Cairns, C. Ferrari, P. Cescon, *Anal. Chem.* 78 (2006) 1883–1886.
- [16] D. Dick, A. Wegner, P. Gabrielli, U. Ruth, C. Barbante, M. Kriews, *Anal. Chim. Acta* 621 (2008) 140–147.
- [17] C. Barbante, G. Cozzi, G. Capodaglio, K. Van de Velde, C. Ferrari, A. Veyssyere, C.F. Boutron, G. Scarponi, P. Cescon, *Anal. Chem.* 71 (1999) 4125–4133.
- [18] F.A.M. Planchon, C.F. Boutron, C. Barbante, E.W. Wolff, G. Cozzi, V. Gaspari, C.P. Ferrari, P. Cescon, *Anal. Chim. Acta* 450 (2001) 193–205.
- [19] M. Krachler, J.C. Zheng, D. Fischer, W. Shtoyk, *Anal. Chim. Acta* 530 (2005) 291–298.
- [20] L.J. Burn-Nunes, P. Vallelonga, R.D. Loss, G.R. Burton, A. Moy, M. Curran, S. Hong, A.M. Smith, R. Edwards, V.I. Morgan, K.J.R. Rosman, *Geochim. Cosmochim. Acta* 75 (2011) 1–20.
- [21] S. Do Hur, T. Soyol-Erdene, H.J. Hwang, C. Han, P. Gabrielli, C. Barbante, C. Boutron, S. Hong, *Glob. Biogeochem. Cycles* 27 (2013), <http://dx.doi.org/10.1002/gbc.20079>.
- [22] E. Korotkikh, P.A. Mayewski, D. Dixon, A.V. Kurbatov, M.J. Handley, *Atmos. Environ.* 89 (2014) 683–687.
- [23] F. Marino, G. Calzolari, S. Caporali, E. Castellano, M. Chiari, F. Lucarelli, V. Maggi, S. Nava, M. Sala, R. Udisti, *Nucl. Instrum. Methods B* 266 (2008) 2396–2400.
- [24] A. Marcelli, D. Hampai, F. Giannone, M. Sala, V. Maggi, F. Marino, F. Pignotti, G. Cibin, *J. Anal. Atmos. Spectrom.* 27 (2012) 33–37.
- [25] D. Hampai, S.B. Dabagov, C. Polese, A. Liedl, G. Cappuccio, *Spectrochim. Acta B* 101 (2014) 114–117.
- [26] D.S. Macholdt, K.P. Jochum, B. Stoll, U. Weis, M.O. Andreae, *Chem. Geol.* 383 (2014) 123–131.
- [27] D. Della Lunga, W. Muller, S.O. Rasmussen, A. Svensson, *J. Glaciol.* 60 (2014) 970–988.
- [28] S.B. Sneed, P.A. Mayewski, W.G. Sayre, M.J. Handley, A.V. Kurbatov, K.C. Taylor, P. Bohleber, D. Wagenbach, T. Erhardt, N.E. Spaulding, *J. Glaciol.* 61 (2015) 233–242.
- [29] G.R.K. Naidu, N. Trautmann, S. Zaunar, T. Balaji, K.S. Rao, *J. Radioanal. Nucl. Chem.* 258 (2003) 421–425.
- [30] E. Witkowska, K. Szczepaniak, M. Biziuk, *J. Radioanal. Nucl. Chem.* 265 (2005) 141–150.
- [31] G. Capannesi, A. Rosada, P. Avino, *Microchem. J.* 93 (2009) 188–194.
- [32] M. Murozumi, T.J. Chow, C. Patterson, *Geochim. Cosmochim. Acta* 33 (1969) 1247–1294.
- [33] A. Wyttenbach, R. Rauter, B. Stauffer, U. Schotterer, *J. Radioanal. Chem.* 38 (1977) 405–413.
- [34] M. Koyama, J. Takada, K. Kamiyama, N. Fujii, J. Inoue, K. Issiki, E. Nakayama, *J. Radioanal. Nucl. Chem.* 124 (1988) 235–249.
- [35] J.R. Petit, M. Briat, A. Royer, *Nature* 293 (1981) 391–394.
- [36] M. Ram, J. Donarummo Jr., M.R. Stolz, G. Koenig, *J. Geophys. Res.* 105 (2000) 24731–24738.
- [37] D.B. Karner, J. Levine, R.A. Muller, F. Asaro, M. Ram, M.R. Stolz, *Geochim. Cosmochim. Acta* 67 (2003) 751–763.
- [38] S.S. Keskin, I. Olmez, *J. Radioanal. Nucl. Chem.* 259 (2004) 199–202.
- [39] R.M. Lindstrom, D.J. Lindstrom, L.A. Slaback, J.K. Langland, *Nucl. Instrum. Methods A* 299 (1990) 425–429.
- [40] T.M. Semkow, P.P. Parekh, C.D. Schwenker, A.J. Khan, A. Bari, J.F. Colaresi, O.K. Tench, G. David, W. Guryn, *Appl. Radiat. Isot.* 57 (2002) 213–223.
- [41] A. Borio di Tigliole, A. Cammi, M. Clemenza, V. Memoli, L. Pattavina, E. Previtali, *Prog. Nucl. Energy* 52 (2010) 494–502.
- [42] M. Clemenza, E. Fiorini, E. Previtali, E. Sala, *J. Environ. Radioact.* 114 (2012) 113–118.
- [43] A. Salvini, M. Clemenza, E. Previtali, A. Borio di Tigliole, M. Cagnazzo, S. Manera, *J. Phys. Conf. Ser.* 41 (2006) 417–423.
- [44] F. Alessandria, et al., CUORE collaboration, *Astropart. Phys.* 35 (2012) 839–849.
- [45] G. Baccolo, N. Maffezzoli, M. Clemenza, B. Delmonte, M. Prata, A. Salvini, V. Maggi, E. Previtali, *J. Radioanal. Nucl. Chem.* 306 (2015) 589–597.
- [46] B. Stenni, et al., TALDICE collaboration, *Nat. Geosci.* 4 (2011) 46–49.
- [47] D. Veres, L. Bazin, A. Landais, A. Toyé Mahamadou Kele, B. Lemieux-Dudon, F. Parrenin, P. Martinerie, E. Blayo, T. Blunier, E. Capron, J. Chappellaz, S.O. Rasmussen, M. Severi, A. Svensson, B. Vinther, E.W. Wolff, *Clim. Past* 9 (2013) 1733–1748.
- [48] B. Delmonte, J.R. Petit, V. Maggi, *Clim. Dynam.* 18 (2002) 647–660.
- [49] A. Borio di Tigliole, A. Cammi, D. Chiesa, M. Clemenza, S. Manera, M. Nastasi, L. Pattavina, R. Ponciroli, S. Pozzi, M. Prata, E. Previtali, A. Salvini, M. Sisti, *Prog. Nucl. Energy* 70 (2014) 249–255.
- [50] R.R. Greenberg, P. Bode, E.A. De Nadai Fernandes, *Spectrochim. Acta B* 66 (2011) 193–241.
- [51] G. Baccolo, M. Clemenza, B. Delmonte, N. Maffezzoli, M. Nastasi, E. Previtali, V. Maggi, *J. Radioanal. Nucl. Chem.* 306 (2015) 429–435.
- [52] L.A. Currie, *Anal. Chem.* 40 (1968) 586–593.
- [53] R. Dams, J.A. Robbins, K.A. Rahn, J.W. Winchester, *Anal. Chem.* 42 (1970) 861–867.
- [54] I. Salma, E. Zemplén-Papp, *Nucl. Instrum. Methods A* 435 (1999) 462–474.
- [55] M.J. Kleeman, J.J. Schauer, G.R. Cass, *Environ. Sci. Technol.* 34 (2000) 1132–1142.
- [56] S.S. Sun, W.F. McDonough, *Geol. Soc. Lond. Spec. Publ.* 42 (1989) 313–345.
- [57] R.L. Rudnick, S. Gao, in: *Treatise on Geochemistry*, vol. 3, Elsevier, 2003, pp. 1–64.
- [58] I. Vlastelic, K. Suchorski, K. Sellegri, A. Colomb, F. Nauret, L. Bouvier, J.L. Piro, *Cosmochim. Geochim. Acta* 167 (2015) 253–268.
- [59] H. Wen, J. Carignan, *Atmos. Environ.* 41 (2007) 7151–7165.
- [60] W.H. Schroeder, J. Munthe, *Atmos. Environ.* 32 (1998) 809–822.
- [61] S. Knusel, D.E. Piguet, M. Schwikowski, H.W. Gaggeler, *Environ. Sci. Technol.* 37 (2003) 2267–2273.
- [62] V. Gaspari, C. Barbante, G. Cozzi, P. Cescon, C.F. Boutron, P. Gabrielli, G. Capodaglio, C. Ferrari, J.R. Petit, B. Delmonte, *Geophys. Res. Lett.* 33 (2006), <http://dx.doi.org/10.1029/2005GL024352>.
- [63] P. Gabrielli, A. Wegner, J.R. Petit, B. Delmonte, P. De Deckker, V. Gaspari, H. Fischer, U. Ruth, M. Kriews, C. Boutron, P. Cescon, C. Barbante, *Quat. Sci. Rev.* 29 (2010) 265–273.
- [64] R.H. Rhodes, J.A. Baker, M.A. Millet, N.A.N. Bertler, *Chem. Geol.* 286 (2011) 207–221.
- [65] B.G. Koffman, M.J. Handley, E.C. Osterberg, M.L. Wells, K.J. Kreutz, *J. Glaciol.* 60 (2014), <http://dx.doi.org/10.3189/2014JG13J137>.
- [66] C. Uglietti, P. Gabrielli, J.W. Olesik, A. Lutton, L.G. Thompson, *Appl. Geochem.* 47 (2014) 109–121.